Effects of depth-dependent viscosity and plate motions on maintaining a relatively uniform mid-ocean ridge basalt reservoir in whole mantle flow

Dave R. Stegman and Mark A. Richards
Department of Earth and Planetary Science, University of California, Berkeley, California, USA

John R. Baumgardner
Theoretical Division, Los Alamos National Laboratory, Los Alamos, New Mexico, USA

Received 25 September 2000; revised 17 August 2001; accepted 22 August 2001; published 18 June 2002.

[1] Mid-ocean ridge basalts (MORBs) exhibit relatively uniform and depleted rare earth element concentrations compared with ocean island basalts (OIBs). Previous researchers have focused on long-term (billion-year timescale) preservation of an enriched and heterogeneous OIB reservoir within the convecting mantle. Such studies commonly conclude that the OIB reservoir must exist in an area which remains isolated from convection, i.e., D''. Here we investigate the maintenance of MORB reservoir homogeneity over shorter timescales in the face of vigorous upper/lower mantle mass exchange (deep subduction), which may be due to two effects: (1) a high-viscosity lower mantle and/or (2) chaotic mixing due to toroidal flow generated by surface plate motions. We explore this conceptual model using three-dimensional spherical numerical models that include surface plate motions, radial viscosity variation, and a geophysically plausible model of mantle density contrasts. A correlation dimension method is used to characterize mixing of passive tracers. For a uniform viscosity mantle the upper and lower mantles mix on essentially the same timescales. A factor of 100 viscosity contrast results in a relative mixing time for the lower mantle only $\sim$30–60% longer than that of the upper mantle. Therefore neither a strong viscosity contrast nor toroidal mixing significantly affects the relative mixing times of the upper and lower mantle. We conclude that return flow from the lower mantle is of similar (depleted) composition and that the depleted MORB source reservoir constitutes most of the mantle, except for a convectively isolated OIB source region at the base of the mantle. *INDEX TERMS:* 8124 Tectonophysics: Earth's interior—composition and state; 8120 Tectonophysics: Dynamics of lithosphere and mantle—general; 1025 Geochemistry: Composition of the mantle; 1010 Geochemistry: Chemical evolution; *KEYWORDS:* mantle mixing, core mantle boundary region

1. Introduction

[2] The trace element geochemistry of basalts that erupted in the world's oceans provides information about the structure and dynamics of the Earth's interior. Basalts that erupted at mid-ocean ridges (MORBs) sample the upper mantle and have a relatively uniform isotopic signature [*Hofmann*, 1997]. The isotopic signature of MORBs also suggests that the upper mantle is well mixed and homogenized on timescales of the order of a few hundred million years [*DePaolo*, 1988]. Ocean island basalts (OIBs) are thought to sample the deep mantle since they are most commonly associated with mantle plumes ascending from the bottom of the mantle [*White*, 1985]. Furthermore, the isotopic signatures of OIBs are highly varied in composition and have been interpreted to be 1 to 2 Gyr old.

0148-0227/02/2001JB000192$09.00

[3] A conventional interpretation of these geochemical data is that there are a number of distinct reservoirs, of which we focus on two: a shallow, homogeneous reservoir that is the source for MORB magmas and a deeper, heterogeneous reservoir that is the source for various OIB magmas. However, seismic tomography indicates that stirring driven by plate subduction occurs over most of the depth of the mantle [*Grand et al.*, 1997; *van der Hilst et al.*, 1997; *Karason and van der Hilst*, 2000], so the persistence of these two reservoirs is puzzling. The most common approach to understanding this paradox has been to attempt to estimate the mixing rate of the mantle over long timescales (billions of years). Some studies have suggested that large portions of the mantle cannot remain isolated due to viscosity stratification over the lifetime of Earth [*van Keken and Zhong*, 1999]. This aspect of the paradox may be explained by a geochemical reservoir at the bottom of the mantle, such as D'', that is isolated from stirring by whole mantle convection. However, the remaining aspect of the

paradox has received far less attention: Why does a homogeneous reservoir persist at the top of the mantle if stirring occurs over the full depth of the mantle?

[4] A model of the mantle flow that is sufficiently layered to prohibit mass exchange between the upper and lower mantle can account for very rapid homogenization of the upper mantle while material in the lower mantle remains isolated for very long timescales [*Richter et al.*, 1982]. However, a strictly layered model of the mantle appears to be in conflict with seismic tomography. Here we consider an alternative whole mantle model in which a mechanism exists to stir the shallow mantle much more quickly relative to stirring of the deeper parts of the mantle [*Gurnis and Davies*, 1986a; *Davies and Richards*, 1992]. Differential mixing of the upper and lower mantle might allow for different regions of the mantle to become relatively more or less mixed without requiring two layers in the mantle that convect separately. Two effects thought to be important for this differential mixing are (1) an increase in viscosity with depth and (2) toroidal flow concentrated in the uppermost mantle due to surface plate motions.

[5] Geophysical observations of the geoid [*Richards and Hager*, 1984], postglacial rebound studies [*Mitrovica and Peltier*, 1995], and the relative fixity of hot spots [*Gurnis and Davies*, 1986b; *Richards*, 1991] suggest that the lower mantle viscosity is at least 1 to 2 orders of magnitude more viscous than the upper mantle. Poloidal flow is represented by divergent and convergent flow at mid-ocean ridges and subduction zones, respectively, and is the main component of flow driven by plate tectonics. However, toroidal flow is generated as well by transform faults, oblique subduction, and plate "spin." This toroidal flow component, an effect which cannot be accounted for in two-dimensional (2-D) geometries, is known to enhance stretching by producing chaotic particle trajectories [*Ferrachat and Ricard*, 1998]. Chaotic particle trajectories can be produced by both a steady flow in 3-D geometry or a time-dependent flow in 2-D geometry (where time is the third dimension required for chaotic flow). Since both plate-motion-generated toroidal flow and the lowest mantle viscosity are concentrated near the surface, the greatest stretching efficiency will occur in the uppermost mantle.

[6] Thus we seek to answer a straightforward question: Can whole mantle flow with (1) depth-dependent viscosity and (2) toroidal flow generated at the surface by plate motions generate such enhanced mixing in the upper mantle that the upper mantle will retain a relatively homogenous composition in the face of whole mantle convection? Put another way, can heterogeneities brought into the upper mantle be mixed almost instantaneously while mixing in the lower mantle occurs at a much slower rate?

[7] To illustrate why different degrees of heterogeneity may occur in the upper and lower mantle, we first consider a simple thought experiment in which there are two boxes of different composition. We assume for simplicity of argument that mixing occurs only in box A and that we can control both the mixing rate and the mass exchange rate with box B. We can define two timescales: τ_r is the residence time of material in box A and can be approximated as the mass of box A divided by the mass exchange rate between boxes A and B, and τ_s is the inverse of the stretching rate, representing the mixing time for box A in isolation.

[8] We now consider the end-member possibilities. If the stretching time is much smaller than the residence time, then material that flows into box A is homogenized quickly and box A can remain homogeneous and compositionally distinct from box B. If, instead, the residence time is much smaller than the stretching time, there is perfect communication between the two boxes and they will quickly take on a mean composition. Here we seek to determine how whole mantle flow associated with plate motions may behave in terms of this simple conceptual framework with box A as the upper mantle and box B as the lower mantle.

2. Quantification of Mixing

[9] At the present time, studies are limited to characterizing mantle mixing from a fluid dynamic perspective by using a proxy method. A typical proxy method employs only a modest number of tracers to characterize mixing in 3-D or 2-D Cartesian geometries. Proxy methods used in previous studies include tracers as strain markers to characterize the stretching efficiency of the entire fluid with only a small number of trajectories [*Kellogg and Stewart*, 1991; *Christensen*, 1989], tracers used in a material line formulation [*Gurnis*, 1986], dividing the region into boxes and counting the number of boxes which contain a given number of tracers [*Schmalzl et al.*, 1996; *Christensen*, 1989; *Ten et al.*, 1997], spectral analysis [*Olson et al.*, 1984], attempting to resolve numerically an interface between two fluids [*Ten et al.*, 1996], and asymptotic methods adapted for use in mantle convection in which only a finite number of overturns occur [*van Keken and Zhong*, 1999; *Spence et al.*, 1988]. In a case such as the present study, in which tracers are advected through a chaotic flow, methods that rely upon the actual trajectories of individual tracers may be unreliable [*Metcalfe et al.*, 1995]; however, it is still possible to use a modest number of tracers to successfully characterize mixing.

[10] To quantify mixing, we have adopted the correlation dimension method [*Schmalzl and Hansen*, 1994] which employs a modest number of tracers and has many advantages over other methods. Aside from the fact that some of the other methods can only be used in a 2-D geometry, the correlation dimension method has two main advantages: (1) We can quantify mixing separately for the upper and lower mantle, and (2) this method gives information about the degree of mixing as a function of length scale. The minimum resolvable length scale depends upon the number of tracers used. The number of calculations required to describe the correlation dimension of each tracer distribution scales as the square of the number of tracers.

[11] The correlation function $H(r)$ is defined as the number of pairs of tracers separated by a distance that is less than a length scale r. If $H(r)$ is approximated as $H(r) = r^{\alpha}$, the exponent α is defined as the correlation dimension. This exponent is essentially the slope of the correlation function when it is plotted on a log scale. The correlation dimension provides information on the dispersion of the tracers. The tracers begin as a point source at time $t = 0$ and asymptotically evolve toward a random distribution at $t = \infty$, when the blob has been homogenized. The more the tracers have been dispersed throughout the volume, the larger the correlation dimension. For length scales very small com-

pared with the size of the spatial domain of interest the correlation dimension of a random distribution of particles approaches a value of 2 in two-dimensional geometry and a value of 3 in three dimensions. However, for length scales approaching the domain dimension (which are of interest in this study) the correlation dimension for a random distribution decreases with increasing length scale (see discussion of Figure 2, section 4). The length scale equal to the size of the box is always the last length scale to reach the completely mixed limit.

3. Description of Models

[12] We use a 3-D spherical model of mantle flow, TERRA [*Baumgardner*, 1985; *Bunge and Baumgardner*, 1995; *Bunge et al.*, 1997], as a numerical fluid dynamical laboratory to investigate mixing in three fluid dynamic models incorporating increasing degrees of realism in simulating plate-scale flow. The first model has a mantle of constant viscosity with flow driven only by imposed surface velocity boundary conditions, which are those of the present-day plate motions. The second model is the same as the first but with a viscosity that increases with depth. The third model includes plate motions and the viscosity contrast of the second model but includes flow driven by internal density heterogeneities due to subduction, commonly referred to as a "slab model" [*Ricard et al.*, 1993; *Lithgow-Bertelloni and Richards*, 1998]. None of these are actually mantle convection models since heat transport does not directly enter the calculations. We are instead treating simpler models that can be used to systematically investigate the effects of surface plates and depth-dependent viscosity on differential mixing times of the upper and lower mantle, the most important simplification being that plate-scale flow dominates mixing in the mantle.

[13] In the first two models we use TERRA to solve the governing equations of mass and momentum conservation subject to the imposed surface plate motions. A confined tracer cloud is inserted into the numerical model, analogous to adding a drop of dye into a tank of fluid. The tracer cloud is inserted near the surface in the instantaneous mantle velocity field. To account for the fact that the imposed surface plate motions will result in chaotic streamlines and therefore a strong sensitivity to initial tracer positions, tracer clouds are inserted at 10 equally spaced locations on the surface of the sphere, and all results presented represent an average of those 10 starting positions. These positions are, for convenience, the equidistant centers of the regular icosahedron from which TERRA's finite element grid is generated [*Baumgardner*, 1985].

[14] The first model has a constant dynamic viscosity mantle of 10^{21} Pa s (the absolute value of viscosity is irrelevant for plate-driven flow), and flow is driven only by present-day surface plate motions. The bottom boundary condition is free slip. There is no barrier of any kind to flow between the upper and lower mantle. This is a minimalist model for mixing, as we do not account for the time variation of plate motions or any subplate-scale modes of convective flow that may occur beneath the plates. Motions imposed by the surface plates cause only limited stirring, and many overturns are required for efficient stirring. The second model is the same as the first but with the addition of a depth-dependent viscosity $\eta_{LM} = 100\eta_{UM}$ in order to study the effects of concentrating stirring (higher strain rates and toroidal flow) in the shallow mantle. The viscosity in the lower 2000 km of the mantle is 10^{23} Pa s, although again, only the viscosity contrast is relevant, not the absolute value. The viscosity increases smoothly with depth beginning at the top of the transition zone (400 km) and reaching the full increase at $\sim$1000 km depth.

[15] The third model includes both features of the previous model and includes internal buoyancy forces arising from the density heterogeneities associated with a history of subduction. A small and insignificant difference is that plate motions are those driven self-consistently by the internal density field, which are only slightly different from those observed [*Lithgow-Bertelloni and Richards*, 1998]. This is a somewhat different viscosity structure than those of Lithgow-Bertelloni and Richards, which had a factor of 30 increase as a step function. These density heterogeneities generate much smaller scale flow, resulting in much more efficient stirring throughout the mantle. Although this is clearly a more realistic model, the resultant velocity field through which tracers are advected is still steady. Thus our models may greatly underestimate absolute mixing rates. However, time-dependent flow probably would not affect the relative mixing rates of the upper and lower mantle, which is the main issue in question in this study.

[16] The particle tracers are advected via a second-order Runge-Kutta method. The accuracy of the velocity field is dependent upon the resolution of the computational mesh. TERRA employs linear shape functions to represent the velocity field in its multigrid finite element treatment, so that second-order interpolation of the velocity field is all that is warranted. For the constant viscosity model the resolution at the surface was 250 km between grid points horizontally and 180 km between grid points radially. For the models with layered viscosity the resolution at the surface was 125 km between grid points horizontally and 90 km between grid points radially. The velocity field is resolved with 125-km grid point spacing since very similar tracer evolutions and resulting correlation dimensions are obtained with the 250-km resolution. The error in tracer position for one revolution around the equator is $\sim 2.0 \times 10^{-5}$ or $\sim$8-km cumulative error for 20 mantle overturn times. Such errors are negligible for the mixing length scales considered below and are similar to errors found in 3-D Cartesian models of similar resolution [*Tackley*, 1998].

4. Results

[17] In Figure 1 a representative evolution of tracers is shown for the kinematic case with constant (Figure 1a) and depth-dependent viscosity (Figure 1b). Tracers are colored to indicate their depth in the mantle relative to other tracers in the distribution. Tracers closest to the surface of the mantle are dark blue, and tracers closest to the core-mantle boundary are red. The core-mantle boundary depth is shown as an orange surface. The initial point source is a cluster of 1352 tracers (a number chosen for convenience in the numerical code) distributed evenly within a small blob of radius 125 km. At the model time shown in Figure 1 the cluster is stirred to the point of having large ribbon-like structures, while a few tracers are dispersed into the larger

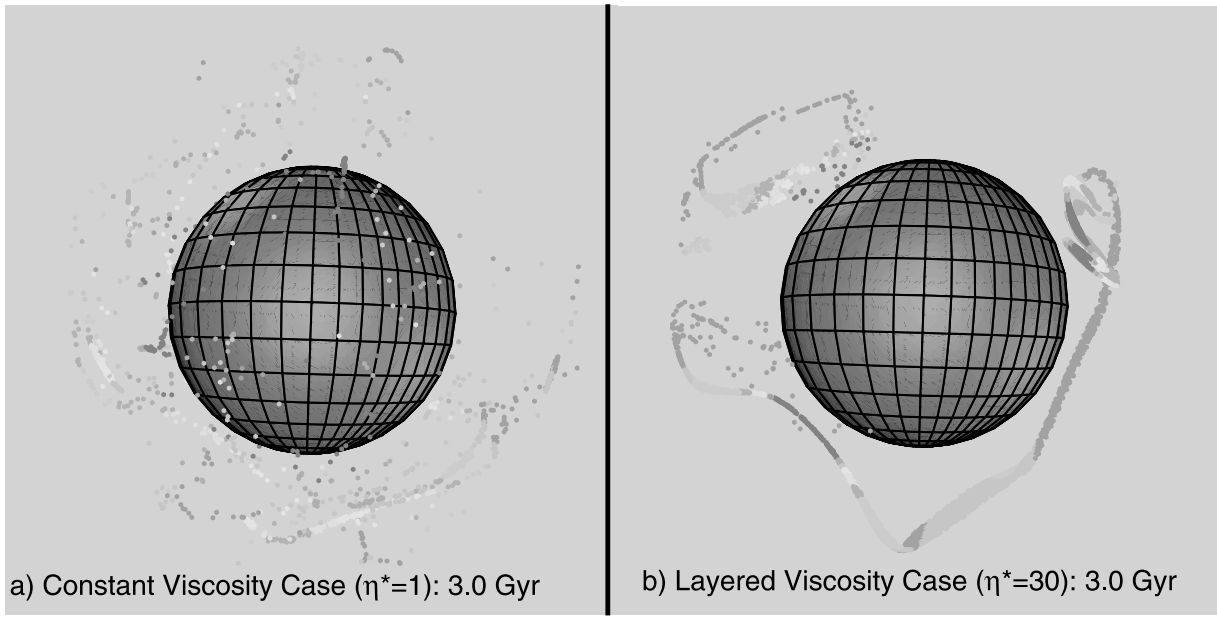

Figure 1. Snapshot of tracer evolution after 3.0 Gyr for (a) a constant viscosity case and (b) a layered viscosity case. In the layered case the lower mantle is 30 times the viscosity of the upper mantle. Color indicates the depth of a tracer relative to all the other tracers in the distribution. Blue tracers are nearest to the surface, and red tracers are closest to the core-mantle boundary. The reference surface shown is at the depth of the core-mantle boundary. The differential mixing effect is seen clearly in Figure 1b, where the leftmost ribbon-like structure is being destroyed by the presence of toroidal flow near the surface. See color version of this figure at back of this issue.

volume. We observe that these features are equally present in both the upper and lower mantle regions. In Figure 1a the only source of mantle stirring is the imposed surface plate motion field (note in Figure 1b the viscosity increase is a factor of 30, which is different from the viscosity increase factor of 100 described in the models and presented in the correlation dimension results that follow).

[18] Since the same surface-velocity boundary condition drives flow in all the models, one is able to compare the absolute mixing times between models that have different viscosity structures. For example, when one compares the same model time for different cases as in Figure 1a (constant viscosity case) and Figure 1b (layered viscosity case), similar amounts of total strain occur in both, but the strain is partitioned differently between the upper and lower mantle.

[19] The nature of stirring caused by the surface motions is best seen in Figure 1b, which shows the evolution of a tracer cloud in a purely kinematic model with a viscosity increase. The plate-scale flow causes the point source to become streaked into large ribbon-like structures, which follow streamlines associated with the large overturning motion. Blue tracers in the far left of the image are part of a ribbon structure that encounters a region of enhanced stirring in the shallow depths of the mantle. This region of enhanced stirring is due to a relatively large toroidal component of the plate motions above. Individual tracers follow paths slightly different than the streak as a whole, as they are dispersed from the ribbon-like structure into a distribution similar to that of a cloud.

[20] This ribbon-like state of dispersion created while the tracers are near the surface is largely preserved by the high-viscosity lower mantle. Such an effect has occurred for the red tracers in the ribbon-like structure just above the core-mantle boundary in the top left portion of Figure 1b. At an earlier model time in the evolution of the ribbon (not shown) that part of the ribbon was near the surface and the tracers were dispersed. Figure 1 illustrates that as expected, surface motions cause stirring concentrated in the upper mantle. The more viscous lower mantle stirs at a much slower rate, largely preserving structures in the state to which they are stirred in the upper mantle.

[21] Before discussing the correlation dimensions obtained in the model experiments we first examine the effective resolution of our method with respect to the number of tracers employed in the calculations. Figure 2 shows the correlation dimension versus length scale obtained from random distributions of 1352, 10,000, and 50,000 tracers within our spherical shell mantle model. At very small length scales the correlation dimension approaches a value of 3 as expected (see curve for 50,000 particles). For length scales of the order of 2000 km or more the correlation dimension appears fairly well resolved even for only 1352 tracers. This is a sufficient minimum horizontal length scale for addressing the relative mixing characteristics of the upper and lower mantle (obviously, the more tracers the better, but in the models discussed in section 3 we were limited by computational resources to single model runs with 1352 tracers each). For comparison, the correlation dimension for 50,000 particles in a (Cartesian) cube of comparable volume is also plotted. Comparing this with the spherical shell result for the same number of particles emphasizes that the "notch" in the spherical shell curve is a feature expected in Earth models that approach a well-mixed state. Note again that the correlation dimension

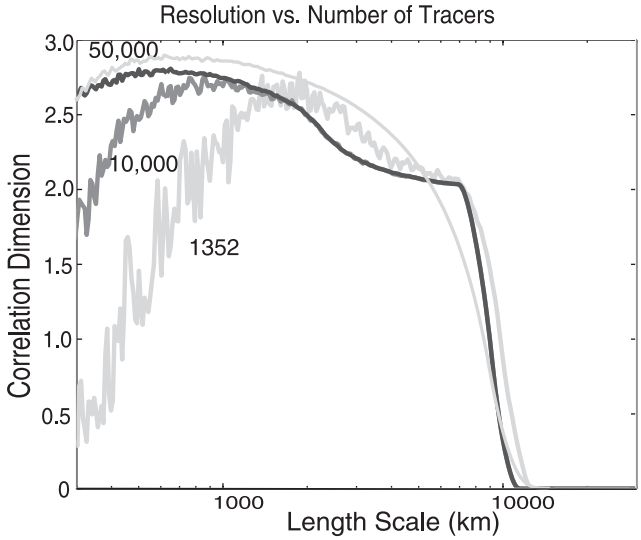

Figure 2. Correlation dimension for random distributions of different numbers of tracers. At very small length scales the random correlation dimension should approach 3 if it is well resolved. The minimum resolvable length scale is defined by the peak in the correlation dimension, which occurs at smaller length scales for a larger number of tracers. For 50,000, 10,000, and 1352 tracers the minimum resolvable length scale is ~600, 900, and 2000 km, respectively. The dashed line shows the correlation dimension for a random distribution of 50,000 tracers in a cube whose diagonal dimension is equal to the radius of Earth.

for wavelengths greater than ~1000 km are significantly less than 3 for random distributions in both Cartesian and spherical shell geometry.

[22] We now proceed to quantify our model results in terms of the correlation dimension. Figure 3 shows the evolution of the correlation dimension of a tracer cloud over time for the kinematic case with constant viscosity. Each curve actually represents an average over 10 equally spaced clouds, as discussed in section 3. Again, only correlation dimensions for length scales of ~2000 km or more are well resolved. The top curve shown is the completely mixed limit, which is the correlation dimension for the entire mantle filled with a random distribution of tracers (using the same number of tracers as used in the models). As expected, the correlation dimension increases with time for all length scales, and given a long enough time, the initial point source tracer distribution becomes indistinguishable from a random distribution. The kinematic model shows that surface plate motions alone are capable of homogenizing an initial point source. The actual times given in Figure 3 may have little direct relevance to Earth, but they describe the evolution of a tracer cloud in a viscous spherical shell with flow entirely driven by a constant (in time) surface plate velocity boundary condition.

4.1. Kinematic Flow With Constant Viscosity

[23] Figure 4a shows the correlation dimension at 1.5 Gyr for both the upper and lower mantle for the constant viscosity model of kinematic flow driven by the surface velocity boundary condition of the present-day plate motions. The distribution of the initial tracer cloud has been separated for those tracers located above 670-km depth (the upper mantle) and those tracers below 670-km depth (the lower mantle). There is no barrier to flow between the upper mantle and lower mantle at 670 km, but the correlation analysis is performed separately in order to characterize the state of mixing in each region. In this way the evolution of a single tracer cloud can simultaneously characterize the degree of mixing for both the upper and lower mantles.

[24] For the 1.5-Gyr tracer distribution, length scales from 2000 to 10,000 km have correlation dimensions for both the upper and lower mantles between 0.3 and 0.6. The velocity field generated by the surface velocity boundary condition causes a bunching of streamlines beneath convergent and divergent boundaries, while the velocity gradients are reduced in the lower mantle. The toroidal component of flow generated by the imposed surface plate motions causes chaotic mixing concentrated in the upper mantle because the toroidal flow component decreases exponentially with depth, with the shorter-wavelength components decaying the most rapidly [*Hager and O'Connell*, 1979].

4.2. Kinematic Flow With Layered Viscosity

[25] Results shown in Figure 4b are for a purely kinematic model with a viscosity that increases with depth

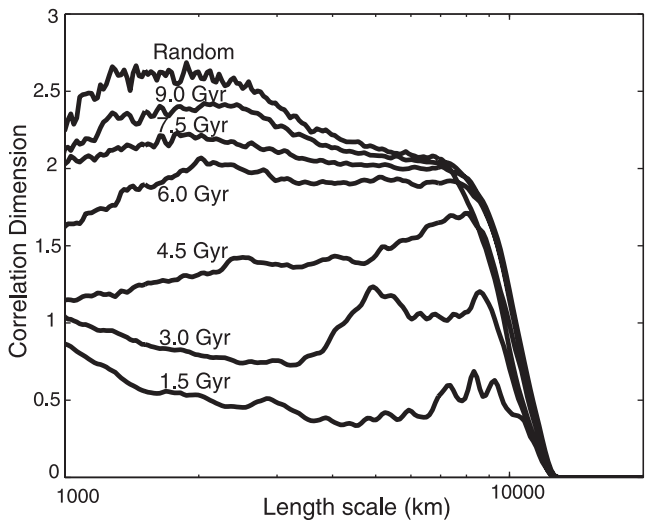

Figure 3. Evolution of a small cluster of 1352 tracers from point source to streak to cloud as quantified by the correlation dimension. The tracer distribution was inserted into the kinematic, constant viscosity model. The top curve is the correlation dimension of a random distribution of the same number of tracers. The tracers distribution evolves toward the random distribution. A correlation dimension equal to 1 is interpreted as having evolved into a streak. This is approximately correct, but as can be seen for the limit of a volume filling cloud, the three-dimensional spherical shell geometry affects the overall shape of the curves. The length scales range from ~2000 km, which is the smallest resolvable length scale when using a modest number of tracers, to ~12,000 km, which is the length scale of the entire volume (diameter of Earth). The state of mixing is described by the correlation dimension of the tracers at a specific length scale at a specific time.

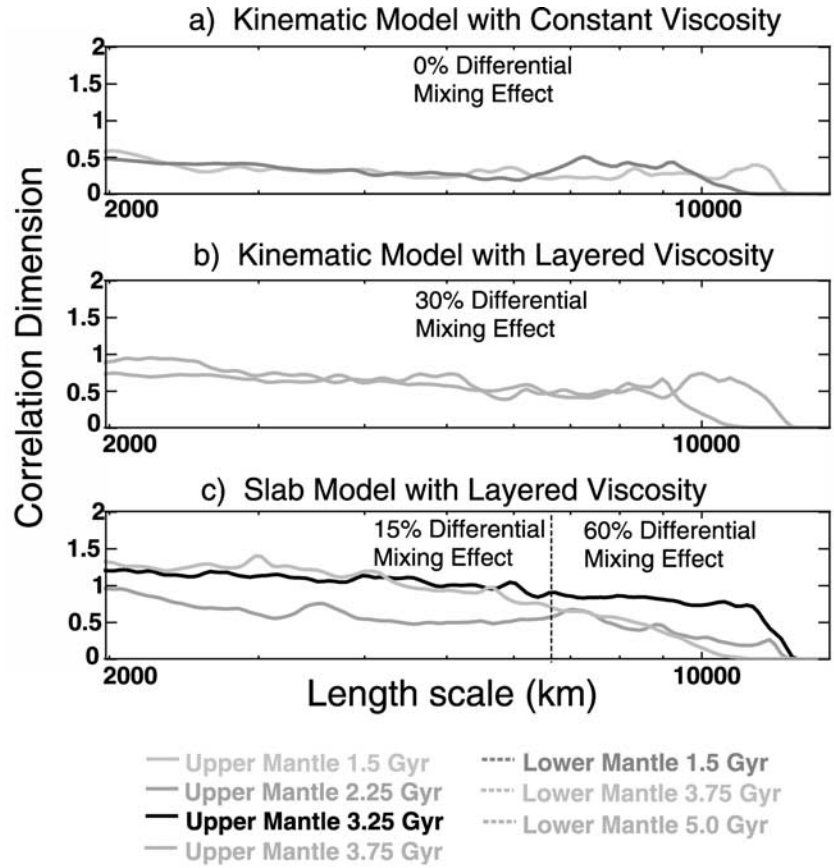

Figure 4. Correlation dimension results for (a) the kinematic model with constant viscosity, (b) the kinematic model with layered viscosity, and (c) the slab model with layered viscosity. See color version of this figure at back of this issue.

through the transition zone by a factor of 100. After 3.75 Gyr of model time the upper mantle attains a correlation dimension between 0.5 and 1.0 at length scales of 2000–9000 km. The lower mantle reaches a correlation dimension between 0.5 and 1.0 after 5.0 Gyr of model time. It takes ~30% longer for the lower mantle to reach the same state of mixing as the upper mantle.

4.3. Flow Driven by Density Heterogeneities With Layered Viscosity

[26] Results are shown in Figure 4c for a model that includes a factor of 100 increase in viscosity with depth, surface plate motions, and internal mantle flow driven by density heterogeneities. As noted in section 3, the surface plate motions in this case are driven self-consistently by the internal density field but differ only slightly from those observed for the present day. After 3.75 Gyr of model time the lower mantle tracers obtain a correlation dimension between 1.0 and 1.5 on length scales smaller than ~6000 km. After 3.25 Gyr of model time for the upper mantle, length scales smaller than 6000 km have also reached similar correlation dimensions between 1.0 and 1.5. At these length scales the upper mantle is mixing only ~15% faster than the lower mantle. However, at length scales of 6000–10,000 km the lower mantle is less mixed than it is at smaller length scales, resulting in correlation dimensions between 0.3 and 1.0. For length scales of 6000–10,000 km the upper mantle obtains correlation dimensions between 0.3 and 1.0 in only 2.25 Gyr. Therefore, at longer (global) length scales the upper mantle becomes mixed ~60% faster than the lower mantle. This model was also studied with a more extreme viscosity layering of a factor of 1000 increase, resulting in relative mixing rates only somewhat slower than those above.

5. Discussion

[27] Referring back to the thought experiment in section 1, the two important quantities that control the degree of differential mixing are the stretching time and the residence time. The residence time is inversely proportional to the mass flux between the upper and lower mantle. We are interested in the regime in which the mantle becomes geochemically layered under conditions of whole mantle flow. This occurs in the limit of "instantaneous mixing," when the residence time is very large or the mass flux is very small. The mass flux between the upper and lower mantle is large and about the same for the three models that we have considered. This means that differences in differ-

ential mixing rates observed in our models are largely a function of the corresponding stretching times.

[28] In order to maintain the relative homogeneity of a reservoir the size of the upper mantle, extreme differential mixing is needed to instantaneously homogenize material coming into the upper mantle from below. Such extreme differential mixing would require mixing in the upper mantle to be at least a factor of 10 times greater than mixing in the lower mantle or a differential mixing effect of at least 1000%. To summarize our results, there was approximately no effect, 30% effect, and 60% effect in the kinematic model with constant viscosity, the kinematic model with layered viscosity, and the slab model, respectively. These effects are too small (by at least 1 order of magnitude) for differential mixing in these models to maintain a homogenous reservoir in the upper mantle that has heterogeneity introduced from the lower mantle.

[29] Our models are useful mainly in evaluating differential mixing times for upper and lower mantle reservoirs, but the absolute mixing rates are clearly underestimated and should be viewed with caution. Flow in the Earth's mantle is time-dependent and includes smaller length scales than are present in our models, which include mainly plate-scale flow. Evidence for small-scale convection in the upper mantle beneath the plates is controversial, but it appears to be unlikely that small-scale flow is responsible for much of the upper mantle heat transport (see *Davies and Richards* [1992] for a more general discussion of this issue). It would nevertheless be interesting to study quantitatively the degree to which a small component of small-scale convection in the uppermost mantle might affect mixing in a mantle otherwise dominated by plate-scale flow.

[30] In this paper we have assumed that the differing degrees of homogeneity and enrichment between OIB and MORB reflect source compositions rather than sampling processes, e.g., greater homogenization and sampling of both enriched and depleted parcels due to more extensive mantle melting at ridges. Although this view is rejected by most geochemists for a variety of reasons, we simply note that it is plausible that both OIB and MORB are derived from the same or similar source rocks via different processes, in which case the need for geochemical distinction between the upper and lower mantle would not be an issue. Models with greater sophistication, such as these including for fractionation effects from partial melting at mid-ocean ridges [*Walzer and Hendel*, 1999] as well as much higher numerical resolution, are needed to test the full range of available hypotheses for mixing in whole mantle convection. In full thermal convection models, in which heat must be transported from the core-mantle boundary through the mantle to the surface, it is likely that maintaining a strong dichotomy in the degree of mixing would be even more difficult.

[31] Seismic tomography indicates that a substantial mass flux occurs across the 670-km discontinuity because many subducted slabs penetrate to great depth in the lower mantle [*Grand et al.*, 1997; *van der Hilst et al.*, 1997]. Also, it is unlikely that the negative Clapeyron slope phase change at 670-km depth is a significant inhibition to radial flow since there is no corresponding large increase in the degree of seismic heterogeneity at that level [*Megnin et al.*, 1997; *Davies*, 1995]. This large mass flux between the upper and lower mantle, combined with the results of our models, suggests that the material of upper mantle composition is representative of all the material in the convecting region and, more specifically, that most of the volume of the mantle is the MORB source reservoir. The OIB reservoir most likely exists outside of the MORB source region, possibly in a layer which is isolated from the convecting region of the mantle (see *Tackley* [2000] for a review of these possibilities). Our conclusions favor the conceptual model of *Coltice and Ricard* [1999], in which most of the mantle is the MORB source region and the enriched, heterogeneous OIB material is contained in a relatively thin layer at the base of the mantle. Subducted oceanic crust has long been proposed as a possible repository for ancient geochemical heterogeneities [*Hofmann and White*, 1982; *Chase*, 1981], and the seismic D'' layer has been proposed to be one place that oceanic crust might segregate [*Christensen and Hofmann*, 1994]. Recent geochemical analysis of OIBs shows that there is indeed a signature of recycled pelagic sediments [*Blichert-Toft et al.*, 1999]. The plausibility of such a model and understanding its dynamics should be a fruitful direction for future work.

[32] **Acknowledgments.** The authors would like to acknowledge the support of NSF and IGPP Los Alamos. We thank Shijie Zhong, Mike Gurnis, and an anonymous reviewer for reviews which strengthened the manuscript and Mark Jellinek, Peter van Keken, and Geoff Davies for helpful comments.

References

Baumgardner, J. R., Three-dimensional finite element model for mantle convection, Ph.D. thesis, Univ. of Calif., Los Angeles, 1985.

Blichert-Toft, I., F. A. Frey, and F. Albarede, Hf isotope evidence for pelagic sediments in the source of Hawaiian basalts, *Science*, *285*, 879–882, 1999.

Bunge, H. P., and J. R. Baumgardner, Mantle convection modeling on parallel virtual machines, *Comput. Phys.*, *9*, 207–215, 1995.

Bunge, H. P., M. A. Richards, and J. R. Baumgardner, A sensitivity study of three-dimensional spherical mantle convection at 10^8 Rayleigh number: Effects of depth-dependent viscosity, heating mode, and an endothermic phase change, *J. Geophys. Res.*, *102*, 11,991–12,007, 1997.

Chase, C. G., Oceanic island Pb: Two-stage histories and mantle evolution, *Earth Planet. Sci. Lett.*, *52*, 277–284, 1981.

Christensen, U., Mixing by time-dependent convection, *Earth Planet. Sci. Lett.*, *95*, 382–394, 1989.

Christensen, U., and A. W. Hofmann, Segregation of subducted oceanic crust in the convecting mantle, *J. Geophys. Res.*, *99*, 19,867–19,884, 1994.

Coltice, N., and Y. Ricard, Geochemical observations and one layer mantle convection, *Earth Planet. Sci. Lett.*, *174*, 125–137, 1999.

Davies, G. F., Penetration of plates and plumes through the mantle transition zone, *Earth Planet. Sci. Lett.*, *133*, 507–516, 1995.

Davies, G. F., and M. A. Richards, Mantle convection, *J. Geol.*, *100*, 151–206, 1992.

DePaolo, D. J., *Neodymium Isotope Geochemistry: An Introduction*, p. 73, Springer-Verlag, New York, 1988.

Ferrachat, S., and Y. Ricard, Regular vs. chaotic mantle mixing, *Earth Planet. Sci. Lett.*, *171*, 75–86, 1998.

Grand, S. P., R. D. van der Hilst, and S. Widiyantoro, Global seismic tomography: A snapshot of convection in the Earth, *GSA Today*, *7*, 1–7, 1997.

Gurnis, M., Stirring and mixing in the mantle by plate-scale flow: Large persistent blobs and long tendrils coexist, *Geophys. Res. Lett.*, *13*, 1474–1477, 1986.

Gurnis, M., and G. F. Davies, The effect of depth-dependent viscosity on convective mixing in the mantle and the possible survival of primitive mantle, *Geophys. Res. Lett.*, *13*, 541–544, 1986a.

Gurnis, M., and G. F. Davies, Numerical study of high Rayleigh number convection in a medium with depth-dependent viscosity, *Geophys. J. Int.*, *85*, 523–541, 1986b.

Hager, B. H., and R. J. O'Connell, Kinematic models of large-scale flow in the Earth's mantle, *J. Geophys. Res.*, *84*, 1031–1048, 1979.

Hofmann, A. W., Mantle geochemistry: The message from oceanic volcanism, *Nature*, *385*, 219–229, 1997.

Hofmann, A. W., and W. M. White, Mantle plumes from ancient oceanic crust, *Earth Planet. Sci. Lett.*, *57*, 421–436, 1982.

Karason, H., and R. D. van der Hilst, Constraints on mantle convection from seismic tomography, in *The History and Dynamics of Global Plate Motions, Geophys. Monogr. Ser.*, vol. 121, edited by M. A. Richards, R. G. Gordon, and R. D. van der Hilst, pp. 277–288, AGU, Washington, D. C., 2000.

Kellogg, L. H., and C. A. Stewart, Mixing by chaotic convection in an infinite Prandtl number fluid and implications for mantle convection, *Phys. Fluids*, *3*, 1374–1378, 1991.

Lithgow-Bertelloni, C., and M. A. Richards, The dynamics of Cenozoic and Mesozoic plate motions, *Rev. Geophys.*, *36*, 27–78, 1998.

Megnin, C., H.-P. Bunge, B. Romanowicz, and M. A. Richards, Imaging 3-D spherical convection models: What can seismic tomography tell us about mantle dynamics?, *Geophys. Res. Lett.*, *24*, 1299–1302, 1997.

Metcalfe, G., C. R. Bina, and J. M. Ottino, Kinematic considerations for mantle mixing, *Geophys. Res. Lett.*, *22*, 743–746, 1995.

Mitrovica, J. X., and W. R. Peltier, Constraints on mantle viscosity based upon the inversion of post-glacial uplift data from the Hudson Bay region, *Geophys. J. Int.*, *122*, 353–377, 1995.

Olson, P., D. A. Yuen, and D. Balsiger, Convective mixing and the fine structure of mantle heterogeneity, *Phys. Earth Planet. Inter.*, *36*, 291–304, 1984.

Ricard, Y., M. Richards, C. Lithgow-Bertelloni, and Y. Le Stunff, A geodynamical model of mantle density heterogeneity, *J. Geophys. Res.*, *98*, 21,895–21,909, 1993.

Richards, M. A., Hotspots and the case for a high-viscosity lower mantle, in *Glacial Isostasy, Sea Level and Mantle Rheology*, edited by R. Sabadini and K. Lambeck, pp. 571–588, Kluwer Acad., Norwell, Mass., 1991.

Richards, M. A., and B. H. Hager, Geoid anomalies in a dynamic Earth, *J. Geophys. Res.*, *89*, 5987–6002, 1984.

Richter, F. M., S. F. Daly, and H.-C. Nataf, A parameterized model for the evolution of isotopic heterogeneities in a convecting system, *Earth Planet. Sci. Lett.*, *60*, 178–194, 1982.

Schmalzl, J., and U. Hansen, Mixing in the Earth's mantle by thermal convection: A scale-dependent phenomenon, *Geophys. Res. Lett.*, *21*, 987–990, 1994.

Schmalzl, J., G. A. Houseman, and U. Hansen, Mixing in vigorous, time-dependent three-dimensional convection and application to the Earth's mantle, *J. Geophys. Res.*, *101*, 21,847–21,858, 1996.

Spence, D. A., J. R. Ockendon, P. Wilmott, D. L. Turcotte, and L. H. Kellogg, Convective mixing in the mantle: The role of viscosity differences, *Geophys. J.*, *95*, 79–86, 1988.

Tackley, P. J., Three-dimensional simulations of mantle convection with a thermochemical basal boundary layer: *D″*?, in *The Core-Mantle Boundary Region, Geodyn. Ser.*, vol. 28, edited by M. Gurnis et al., pp. 231–253, AGU, Washington, D. C., 1998.

Tackley, P. J., Mantle convection and plate tectonics: Toward an integrated physical and chemical theory, *Science*, *288*, 2002–2007, 2000.

Ten, A., D. A. Yuen, T. B. Larsen, and A. V. Malevsky, The evolution of material surfaces in convection with variable viscosity as monitored by a characteristics-based method, *Geophys. Res. Lett.*, *23*, 2001–2004, 1996.

Ten, A., D. A. Yuen, Y. Y. Podladchikov, T. B. Larsen, E. Pachepsky, and A. V. Malevsky, Fractal features in mixing of non-Newtonian and Newtonian mantle convection, *Earth Planet. Sci. Lett.*, *146*, 401–414, 1997.

van der Hilst, R. D., S. Widiyantoro, and E. R. Engdahl, Evidence for deep mantle circulation from global tomography, *Nature*, *386*, 578–584, 1997.

van Keken, P., and S. J. Zhong, Mixing in a 3-D spherical model of present-day mantle convection, *Earth Planet. Sci. Lett.*, *171*, 533–547, 1999.

Walzer, U., and R. Hendel, A new convection-fractionation model for the evolution of principal geochemical reservoirs of the Earth's mantle, *Phys. Earth Planet. Inter.*, *112*, 211–256, 1999.

White, W. M., Sources of Oceanic basalts: Radiogenic isotope evidence, *Geology*, *13*, 115–118, 1985.

J. R. Baumgardner, Theoretical Division, Los Alamos National Laboratory, MS B216, Los Alamos, NM 87545, USA. (baumgardner@lanl.gov)

M. A. Richards and D. R. Stegman, Department of Earth and Planetary Science, University of California, 307 McCone Hall, Berkeley, CA 94720, USA. (markr@seismo.berkeley.edu; dstegman@seismo.berkeley.edu)

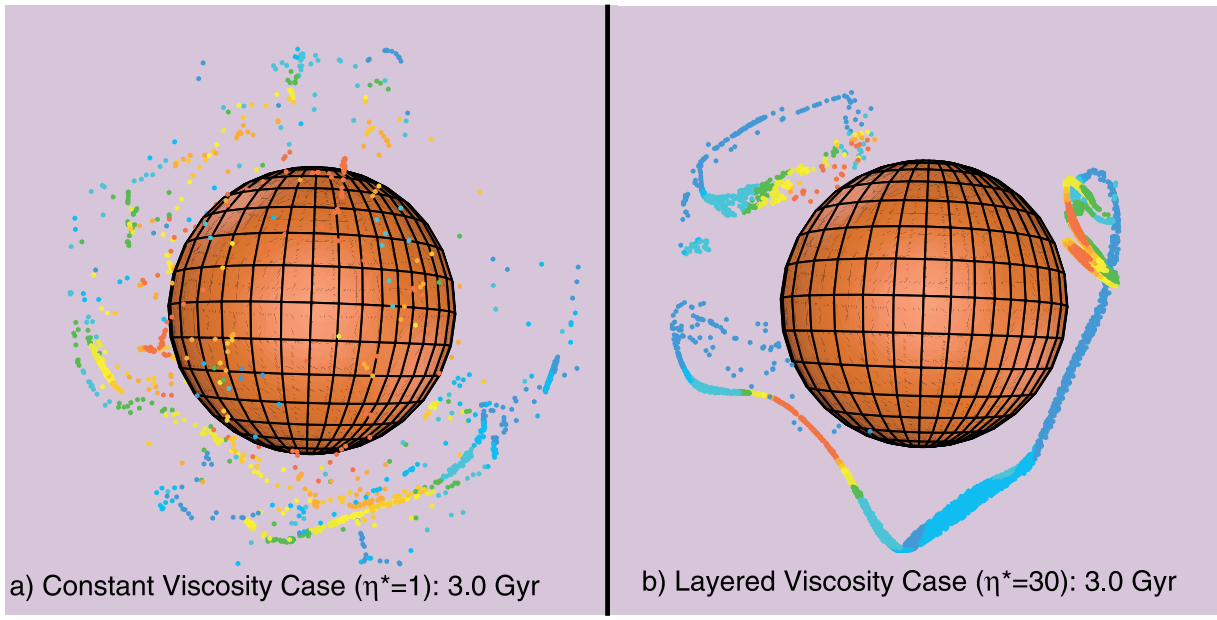

Figure 1. Snapshot of tracer evolution after 3.0 Gyr for (a) a constant viscosity case and (b) a layered viscosity case. In the layered case the lower mantle is 30 times the viscosity of the upper mantle. Color indicates the depth of a tracer relative to all the other tracers in the distribution. Blue tracers are nearest to the surface, and red tracers are closest to the core-mantle boundary. The reference surface shown is at the depth of the core-mantle boundary. The differential mixing effect is seen clearly in Figure 1b, where the leftmost ribbon-like structure is being destroyed by the presence of toroidal flow near the surface.

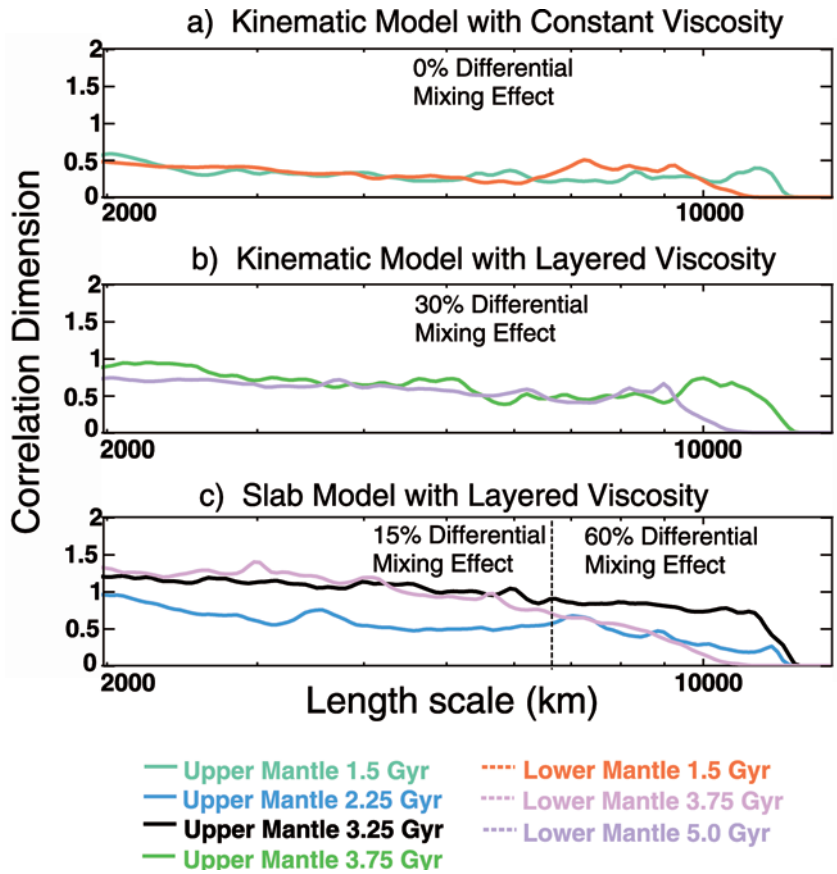

Figure 4. Correlation dimension results for (a) the kinematic model with constant viscosity, (b) the kinematic model with layered viscosity, and (c) the slab model with layered viscosity.